Scrapie infection and endogenous retroviral expression in sheep lymphoid tissues.

Scrapie infection and endogenous retroviral expression in sheep lymphoid tissues.

M.K.F. Salamat, A. Gossner, B. Bradford, N. Hunter, J. Hopkins, & F. Houston*

Division of Infection and Immunity, The Roslin Institute, R(D)SVS, University of Edinburgh, Easter Bush, Midlothian, EH25 9RG, UK.

Abstract

(200 words)

Transmissible spongiform encephalopathies, or prion diseases, are fatal neurodegenerative diseases affecting humans and animals. Although many host tissues express PrP^{C} (essential for prion replication), relatively few cell types accumulate significant levels of infectivity, including neurons and other cell types in the nervous system, and follicular dendritic cells in secondary lymphoid organs. This suggests that tissue or cell-specific receptors or cofactors could play a role in controlling differential susceptibility to infection. Endogenous retroviruses (ERV), the remnants of ancient retroviral integration into the host germline, may represent one such cofactor. We examined the effect of scrapie infection on expression of three ovine ERV families (enJSRV/β1-OERV, γ1-OERV, γ2-OERV) in secondary lymphoid tissues of sheep at different time points following subcutaneous inoculation, using RT-qPCR. These OERVs were constitutively expressed in the prescapular lymph node and spleen of uninfected sheep. However, we were unable to find convincing evidence of specific differential expression of OERV in the same tissues following scrapie infection, in contrast to previous studies of ERV expression in brains of prion-infected mice and macaques. This study is the first to quantify the expression of potentially functional OERV transcripts in sheep lymphoid tissues, opening up interesting questions about the consequences for host immune function.

Abbreviations:

ERV, endogenous retrovirus; OERV, ovine ERV; HERV, human ERV; TSE, transmissible spongiform encephalopathy; PrP^{SC}, disease-associated form of prion protein, Sc for scrapie; RT-qPCR, reverse transcription quantitative polymerase chain reaction; PSLN, prescapular lymph node.

* Corresponding author: Fiona Houston (fiona.houston@roslin.ed.ac.uk)

Introduction:

Prions are lethal infectious agents that cause transmissible neurodegenerative disorders including Creutzfeldt-Jakob disease (CJD) in humans, bovine spongiform encephalopathy in cattle and scrapie in sheep and goats. A key feature in their development is the accumulation of a conformationally altered and aggregated isoform (PrP^{Sc}, Sc for scrapie) of the naturally occurring host-encoded prion protein (PrP^{C}, c for cellular form) in the brains of infected individuals; accompanied by neurodegenerative changes, including neuronal loss, and astrogliosis, which result in the clinical manifestations of the disease. Prion replication appears to rely on a process of seeded polymerization, whereby PrP^{Sc} aggregates bind PrP^{C} and catalyse its conversion to the misfolded form of the protein. In some diseases such as scrapie, chronic wasting disease and variant CJD, prion replication occurs not only in the central nervous system, but also in the lymphoreticular tissues, with follicular dendritic cells as the major reservoir. Although lymphoid prion replication is not associated with overt pathology, it appears to play an important role in neuroinvasion, and in shedding/transmission of infection through direct contact and environmental contamination (animals) or routes such as blood transfusion (humans) (Houston and Andreoletti, 2019). However, little is known about the molecular mechanisms and specific cellular cofactors that determine prion tissue tropism and replication *in vivo*. Several lines of evidence point to interactions between prions and both exogenous and endogenous retroviruses (ERV). Endogenous retroviruses are remnants of past integrations of exogenous retroviruses into the host germline, and form a significant proportion of transposable elements in the genome of most mammalian species (Johnson, 2019). Initially, scrapie infection was shown to activate the expression of endogenous murine leukaemia viruses (MuLV) in the central nervous system of a senescence accelerated mouse strain, SAMP8, and it was suggested that MuLV might accelerate the progression of scrapie pathogenesis (Carp et al., 1999; Lee et al., 2006; Lee et al., 2013). Co-infection of cell lines with scrapie and exogenous retroviruses, such as Moloney MuLV or a small ruminant lentivirus, resulted in enhanced accumulation and/or release of PrP^{Sc} and infectivity from cells (Leblanc et al., 2006; Stanton et al., 2008). Scrapie infection of two neuronal cell lines was shown to influence murine ERV expression, and treatment of the cell lines with the anti-prion drug pentosan polysulphate suppressed scrapie-induced MuLV expression (Stengel et al., 2006). Increased expression of class-I endogenous gamma-retroviruses has been observed in the brains of BSE-infected cynomolgus macaques (Greenwood et al., 2011), and elevated levels of specific human ERV families (HERV-L and HERV-W) were found in cerebrospinal fluid of sporadic CJD patients (Jeong et al., 2010; Lee et al., 2013). It is still unclear whether the observed changes of ERV expression during *in vitro* and *in vivo* prion infection are a cause or consequence of the infection, but it can be hypothesized that

endogenous retroviral elements may contribute to prion disease pathogenesis directly, or indirectly through effects on prion replication.

To date, the interaction between prion infection and ERV in lymphoid tissues has not been studied. In mice, it has been shown that immune stimulation can result in the appearance of endogenous MuLV particles in follicular dendritic cells, and that PrP^C appears to downregulate their expression (Lotscher et al., 2007). Sheep represent a good model to study the association between prion infection and ERV expression in lymphoid tissues, since they are a natural host of scrapie with extensive replication of the infectious agent in secondary lymphoid tissues. The sheep genome also contains at least 27 copies of endogenous β-retroviruses (enJSRV or β1-OERV), which are highly related to their exogenous pathogenic counterpart, Jaagsiekte sheep retrovirus (JSRV), the cause of a transmissible lung cancer (Armezzani et al., 2014; Cumer et al., 2019; Garcia-Etxebarria et al., 2014; Spencer and Palmarini, 2012). In addition, two endogenous class II gamma-retrovirus families (γ1-OERV and γ2-OERV) that produce functional transcripts have been identified in sheep, and classified as members of the murine leukemia virus-like superfamily (Klymiuk et al., 2003). The expression and function of OERV in sheep lymphoid tissues has not been extensively investigated, apart from one study of enJSRV mRNA expression in immune organs (spleen and thymus) of foetal and newborn lambs (Qi et al., 2012). The aim of our study was to determine the effect of scrapie infection on expression of sheep endogenous retroviruses in secondary lymphoid tissues using an experimental infection model.

Materials and Methods:

Sheep with two different *PRNP* genotypes (VRQ/VRQ, ARR/ARR) were experimentally infected by subcutaneous injection of the experimental scrapie isolate SSBP/1 in the neck, as described in a previous study (Gossner et al., 2011). VRQ/VRQ sheep are highly susceptible to infection and show extensive PrP^{Sc} deposition in lymphoid tissues, while ARR/ARR sheep appear completely resistant to infection with SSBP/1 (no clinical disease, and no detectable PrP^{Sc} deposits in brain and lymphoid tissues). For each genotype, groups of three infected sheep and two negative controls (injected with normal sheep brain homogenate) were killed at different time points post infection and brain and lymphoid tissues were collected for analysis. Tissue samples were collected in RNAlater (Ambion) and stored at -80°C. Details of the incubation periods, pathological changes and tissue-specific changes in gene expression can be found in previous publications (Gossner et al., 2011). The levels of enJSRV/β1-, γ1- and γ2–OERV in spleen and prescapular lymph node (PSLN) were measured using reverse transcription quantitative polymerase chain reaction (RT-qPCR). Total RNA was extracted from spleen and prescapular lymph nodes and first strand cDNA synthesized using random hexamer primers. Preparations of cDNA were diluted to normalize starting concentrations, and RT-qPCR were performed

(more details in Supplementary material) using published primers (Table S1) for ERV amplification (Black et al., 2010; Klymiuk et al., 2003). Briefly, the primers for β-OERV amplified *env* and the U3 region of the long terminal repeat (LTR) of all members of the enJSRV/β1-OERV family, whereas those for those for the two γ-OERV families (γ1-OERV and γ2-OERV) amplified the *pro*/*pol* region. Reference genes selected SDHA (succinate dehydrogenase complex flavoprotein subunit A) and tyrosine 3-monooxygenase/tryptophan 5-monooxygenase activation protein zeta (YWHAZ) had previously been screened and published (Gossner et al., 2009). However after initial screening, SDHA was selected for normalization with cDNA derived from the PSLN and spleen in this study, as it is commonly used for both the tissues.

Sheep genomic DNA as positive control and a reaction with no template (NTC) as negative control were included in each run. Relative expression levels were quantified from at least two different cDNA preparations in separate qPCR runs, each time using cDNA from a different RT reaction, and within a run each sample was assayed in duplicate. The relative efficiencies of the target and reference amplification were measured by running standard curves for each amplicon using the same sample. For valid relative or comparative quantification (ΔΔCt method), the efficiency of the target amplicon and of the reference gene must be approximately equal as an ideal efficiency will allow perfect doubling of amplicon in each cycle. This was achieved by running standard curves for each amplicon using the same sample. The Ct values were normalized to the levels of the reference genes. Linear regression analysis of OERV RNA expression levels in negative control animals did not show any continuous trends over time in the susceptible genotype, and no effect of time in resistant genotype (Figure S1 and Table S2). We therefore grouped ΔCt values for negative control animals from all time-points together for calculation of relative average gene expression and applied statistical analysis. Expression levels in scrapie-infected sheep were determined relative to expression in negative control animals using the ΔΔCt method. To calculate relative gene expression levels in infected sheep at a given time point, gene expression data were normalized so that the mean expression level of each gene of interest in all mock-infected control sheep was 1.0. Data are presented as relative gene expression, infected vs mock-infected ± SD. Statistical analyses were performed using IBM SPSS Statistics 24 or GraphPad Prism 8.0 software (GraphPad Software, La Jolla, CA, USA) on log converted ΔCt values and values of $P < 0.05$ were accepted as significant and data. We performed multiple comparison of OERV expression levels at different time points by one-way ANOVA, and where this showed a statistically significant result ($p < 0.05$), we performed post-hoc Tukey's tests to find the time points at which mean OERV expression level in infected animals were significantly different from negative control animals.

Results and Discussion:

Analysis of the spleen and lymph node samples from all mock-infected negative controls revealed that total RNA for β1-OERV family, γ1-OERV and γ2-OERV are constitutively expressed, although expression levels were quite variable, with very low levels (100-1000 fold less than reference genes) of OERV transcripts in some individuals (Figure 1 and Figure S1). On average, expression of β1- and γ1-OERV was consistently lower than that of the reference gene, while expression of γ2-OERV was slightly higher. There were no significant differences in expression levels between spleen and prescapular lymph node, or between scrapie susceptible (VRQ/VRQ) and scrapie resistant (ARR/ARR) sheep.

The sheep were inoculated by subcutaneous injection of scrapie-infected brain homogenate (SSBP/1) in the side of the neck, an area with lymphatic drainage to the prescapular lymph node (PSLN), and PrP^{Sc} deposits were first detected in the PSLN at 25 days post infection (dpi) in VRQ/VRQ sheep (Gossner et al., 2009). This was followed by spread of infection to other lymphoid tissues, with PrP^{Sc} detected in the spleen at 75 days post infection in VRQ/VRQ sheep. Expression of β1-, γ1- and γ2-OERV in the PSLN and spleen was analyzed by RT-qPCR at different time points following infection (Figures 2 and S2).

In the prescapular lymph node of scrapie-infected VRQ/VRQ sheep, one-way ANOVA showed no statistically significant differences in transcription of β-OERV or γ1-OERV relative to mock-infected controls during the course of infection (Figure 2). For γ2-OERV, ANOVA indicated there was a statistically significant difference between negative controls (independent) and infected time-points (dependent variable), however Tukey's post-hoc tests did not identify statistically significant differences for any individual time points. Analysis of OERV relative gene expression in PSLN samples from scrapie-resistant ARR/ARR sheep challenged with scrapie showed statistically significant differences by one-way ANOVA for β-OERV and γ1-OERV, but post-hoc tests identified a statistically significant difference only for β-OERV at 100 dpi (3.5 fold increase , p=0.01) (Figure 2).

Similar results were obtained following analysis of OERV expression in the spleen of scrapie-infected sheep (Figure S2). In scrapie-susceptible VRQ/VRQ sheep, there was a statistically significant increase in relative expression of γ1-OERV at 125 dpi (2.5, p=<0.001) only. In scrapie-resistant ARR/ARR sheep, statistically significant changes in relative expression of β-OERV were found by post-hoc tests at two time points, 50 dpi (2.26 fold increase, p=0.04) and 100 dpi (2.83 fold increase, p=0.001), and in γ1-OERV expression at 10 dpi (2.14 fold increase, p=0.04).

Taken together, the results do not reveal a consistent pattern of differential regulation of OERV expression in lymphoid tissues following scrapie infection in sheep. In scrapie-susceptible VRQ/VRQ

sheep, only γ1-OERV showed a statistically significant increase in expression in spleen at one time point (125 dpi), which coincided with the detection of PrP^{Sc} deposition by immunohistochemistry. However, statistically significant changes in expression of β-OERV and γ1-OERV were also observed at various time points in spleen and/or PSLN samples from scrapie resistant ARR/ARR sheep challenged with scrapie. Since there is no evidence of active replication of the scrapie agent in sheep of this genotype, it is therefore possible that statistically significant differences in gene expression in both VRQ/VRQ and ARR/ARR animals may not be specifically associated with the presence and/or replication of prions.

The reasons for this outcome are undoubtedly related to the large variation in levels of OERV expression in the lymphoid tissues of uninfected sheep, with some samples showing high (20-30 fold greater), and others very low or undetectable (100-1000 fold lower) levels of transcripts (Figure 1 and S1) compared to the reference gene. With only three scrapie-infected sheep per time point, similar variability in OERV expression levels in these individuals could lead to apparently statistically significant differences in relative gene expression arising by chance. To resolve the question of whether OERV expression in lymphoid tissues changes following scrapie infection, it would be necessary to repeat the experiment using larger numbers of biological replicates.

Relatively little is known about tissue-specific expression and regulation of OERV, and this study represents the first substantial effort to quantify expression of OERV RNA in secondary lymphoid tissues of normal adult sheep (negative mock-infected controls). In previous studies, expression of enJSRV/β1-OERV mRNA was detected in lung, kidney, thymus, bone marrow, spleen, mediastinal lymph node, and leucocytes of adult sheep by PCR (Palmarini et al., 1996). In foetal and neonatal lambs, enJSRV/β1-OERV expression was shown to be significantly upregulated in thymus, spleen and mesenteric lymph node during development (Qi et al., 2012). PCR analysis also demonstrated expression of γ1- and γ2-OERV families in heart, spleen, kidney, liver, lung and thymus of foetal and adult sheep but, interestingly, not in peripheral blood mononuclear cells (Klymiuk et al., 2003). Our data suggests that β1-, γ1- and γ2-OERV families are constitutively expressed in spleen and prescapular lymph node of adult sheep, although there is considerable inter-individual variation in expression levels. The estimated copy number of γ2-OERV sequences in the sheep genome (>100 copies per haploid genome) is greater than those of γ1- and β1-OERV sequences (approximately 25 copies each) (Klymiuk et al., 2003), and this may partly explain the higher levels of γ2-OERV RNA expression seen in our experiments.

The majority of ERV sequences incorporated into host genomes are inactivated by host epigenetic silencing or mutations, deletions and recombination events which disrupt the viral open reading

frames (ORF). However, there are numerous examples of the retention of partial or complete ERV sequences with intact ORF over extended evolutionary time periods, suggesting that they have co-evolved with the host to perform beneficial physiological functions. Among the best known examples of this is the role of ERV-derived *Env* proteins (syncytins) in placental development, which appears to have arisen from independent retroviral integration events in several different species (Imakawa et al., 2015). There is also accumulating evidence that ERV may have beneficial roles in maintenance and modulation of host immune responsiveness, as well as contributing to the pathogenesis of immune disorders (Chuong et al., 2016; Kassiotis and Stoye, 2016). In our study, we have demonstrated transcription of three OERV families known to retain retroviral ORF in two secondary lymphoid tissues of sheep, but the mechanisms regulating transcription and functional consequences for the host are not clear. Immune activation has been shown to induce expression of endogenous retroelements including ERV (Lotscher et al., 2007; Young et al., 2014; Zeng et al., 2014), and since secondary lymphoid tissues are the major sites for induction of adaptive immune responses, this may partly explain the observed expression of OERV in these tissues. Further work will be necessary to determine which cell types within lymphoid tissues express OERV, and whether OERV-derived proteins or nucleic acids influence the normal function of the sheep immune system.

Previous studies in scrapie-infected mice and BSE-infected macaques demonstrated induction or activation of ERV expression in areas of the brain with neuropathological lesions, but it was not clear whether this contributed to disease pathogenesis. However, evidence is accumulating that ERV play a role in the development of a number of different neurological diseases. For example, expression of the human endogenous retrovirus HERV-K is increased in the brain of patients with amyotrophic lateral sclerosis (ALS), and mice expressing the HERV-K Env gene develop symptoms of ALS, showing that neurotoxic effects of ERV proteins may contribute to neurodegeneration (Li et al., 2015). The relationship between prion infection and ERV expression in lymphoid tissues has not previously been studied to our knowledge. We were unable to find strong evidence of differential expression of OERV associated with scrapie infection of lymphoid tissues in sheep. This may be due to small sample sizes and inter-individual variability in OERV expression, meaning that the study did not have sufficient statistical power to detect genuine differences in expression between infected and control animals. In addition, the primers used were designed to amplify closely related sequences in β1-, γ1- and γ2-OERV families, therefore if scrapie infection induced differential expression of only one or two individual OERV, the method may not be sufficiently sensitive to detect this. It is also possible that scrapie infection of sheep lymphoid tissues does not induce changes in expression of OERV, since there are known to be tissue-specific differences in regulation of ERV expression (Taruscio and Mantovani, 2004). Further investigation using larger numbers of animals or *in vitro* cell/tissue culture systems may

help to resolve this question. Activation of ERV in lymphoid tissues of prion-infected animals, if detected, could have very different effects on disease pathogenesis than ERV expression in the brain, since prion infection of lymphoid tissues generally does not result in any overt pathology. Rather, it is possible that ERV expression in lymphoid tissues could contribute to dissemination or transmission of prions within and between hosts. The intriguing relationship between ERV and prions deserves further exploration to determine whether ERV may be an important host co-factor in prion propagation.

Funding information

This project was funded by the UK Biotechnology and Biological Sciences Research Council (BBSRC – award reference BBS/E/D/20251968).

Acknowledgements

The authors would like to acknowledge staff from the Animal Services division at the BBSRC Institute for Animal Health, Compton (now the Pirbright Institute) for their care of the sheep and assistance with post mortem sample collection. We would like to thank Dr Alessio Alfieri for assistance in optimization of RT-qPCR, and Dr Darren Shaw and Miss Rida Ayyaz for help with statistical analysis.

Conflicts of interest

All the authors declare no competing interests.

Ethical statement

Animal experiments were approved by the Animal Welfare and Ethics Committee of the BBSRC Institute for Animal Health, and performed under the authority of a Home Office Project Licence (PPL 60/02192).

Armezzani, A., Varela, M., Spencer, T.E., Palmarini, M., Arnaud, F., 2014. "Menage a Trois": the evolutionary interplay between JSRV, enJSRVs and domestic sheep. Viruses 6, 4926-4945.
Black, S.G., Arnaud, F., Burghardt, R.C., Satterfield, M.C., Fleming, J.A., Long, C.R., Hanna, C., Murphy, L., Biek, R., Palmarini, M., Spencer, T.E., 2010. Viral particles of endogenous betaretroviruses are released in the sheep uterus and infect the conceptus trophectoderm in a transspecies embryo transfer model. Journal of virology 84, 9078-9085.
Carp, R.I., Meeker, H.C., Caruso, V., Sersen, E., 1999. Scrapie strain-specific interactions with endogenous murine leukaemia virus. The Journal of general virology 80 (Pt 1), 5-10.
Chuong, E.B., Elde, N.C., Feschotte, C., 2016. Regulatory evolution of innate immunity through co-option of endogenous retroviruses. Science (New York, N.Y.) 351, 1083-1087.
Cumer, T., Pompanon, F., Boyer, F., 2019. Old origin of a protective endogenous retrovirus (enJSRV) in the Ovis genus. Heredity 122, 187-194.
Garcia-Etxebarria, K., Sistiaga-Poveda, M., Jugo, B.M., 2014. Endogenous retroviruses in domestic animals. Current genomics 15, 256-265.
Gossner, A., Roupaka, S., Foster, J., Hunter, N., Hopkins, J., 2011. Transcriptional profiling of peripheral lymphoid tissue reveals genes and networks linked to SSBP/1 scrapie pathology in sheep. Veterinary microbiology 153, 218-228.
Gossner, A.G., Bennet, N., Hunter, N., Hopkins, J., 2009. Differential expression of Prnp and Sprn in scrapie infected sheep also reveals Prnp genotype specific differences. Biochemical and biophysical research communications 378, 862-866.
Greenwood, A.D., Vincendeau, M., Schmadicke, A.C., Montag, J., Seifarth, W., Motzkus, D., 2011. Bovine spongiform encephalopathy infection alters endogenous retrovirus expression in distinct brain regions of cynomolgus macaques (Macaca fascicularis). Molecular neurodegeneration 6, 44.
Houston, F., Andreoletti, O., 2019. Animal prion diseases: the risks to human health. Brain pathology (Zurich, Switzerland) 29, 248-262.
Imakawa, K., Nakagawa, S., Miyazawa, T., 2015. Baton pass hypothesis: successive incorporation of unconserved endogenous retroviral genes for placentation during mammalian evolution. Genes to cells : devoted to molecular & cellular mechanisms 20, 771-788.
Jeong, B.H., Lee, Y.J., Carp, R.I., Kim, Y.S., 2010. The prevalence of human endogenous retroviruses in cerebrospinal fluids from patients with sporadic Creutzfeldt-Jakob disease. Journal of clinical virology : the official publication of the Pan American Society for Clinical Virology 47, 136-142.
Johnson, W.E., 2019. Origins and evolutionary consequences of ancient endogenous retroviruses. Nature reviews. Microbiology 17, 355-370.
Kassiotis, G., Stoye, J.P., 2016. Immune responses to endogenous retroelements: taking the bad with the good. Nature reviews. Immunology 16, 207-219.
Klymiuk, N., Muller, M., Brem, G., Aigner, B., 2003. Characterization of endogenous retroviruses in sheep. Journal of virology 77, 11268-11273.
Leblanc, P., Alais, S., Porto-Carreiro, I., Lehmann, S., Grassi, J., Raposo, G., Darlix, J.L., 2006. Retrovirus infection strongly enhances scrapie infectivity release in cell culture. The EMBO journal 25, 2674-2685.
Lee, K.H., Jeong, B.H., Jin, J.K., Meeker, H.C., Kim, J.I., Carp, R.I., Kim, Y.S., 2006. Scrapie infection activates the replication of ecotropic, xenotropic, and polytropic murine leukemia virus (MuLV) in brains and spinal cords of senescence-accelerated mice: implication of MuLV in progression of scrapie pathogenesis. Biochemical and biophysical research communications 349, 122-130.
Lee, Y.J., Jeong, B.H., Choi, E.K., Kim, Y.S., 2013. Involvement of endogenous retroviruses in prion diseases. Pathogens (Basel, Switzerland) 2, 533-543.
Li, W., Lee, M.H., Henderson, L., Tyagi, R., Bachani, M., Steiner, J., Campanac, E., Hoffman, D.A., von Geldern, G., Johnson, K., Maric, D., Morris, H.D., Lentz, M., Pak, K., Mammen, A., Ostrow, L.,

306 Rothstein, J., Nath, A., 2015. Human endogenous retrovirus-K contributes to motor neuron
307 disease. Science translational medicine 7, 307ra153.
308 Lotscher, M., Recher, M., Lang, K.S., Navarini, A., Hunziker, L., Santimaria, R., Glatzel, M., Schwarz, P.,
309 Boni, J., Zinkernagel, R.M., 2007. Induced prion protein controls immune-activated
310 retroviruses in the mouse spleen. PloS one 2, e1158.
311 Palmarini, M., Cousens, C., Dalziel, R.G., Bai, J., Stedman, K., DeMartini, J.C., Sharp, J.M., 1996. The
312 exogenous form of Jaagsiekte retrovirus is specifically associated with a contagious lung
313 cancer of sheep. Journal of virology 70, 1618-1623.
314 Qi, J.W., Wu, X.L., Liu, S.Y., Cao, G.F., 2012. Expression of endogenous beta retroviruses and Hyal-2
315 mRNA in immune organs of fetuses and lambs. Virologica Sinica 27, 83-92.
316 Spencer, T.E., Palmarini, M., 2012. Endogenous retroviruses of sheep: a model system for
317 understanding physiological adaptation to an evolving ruminant genome. The Journal of
318 reproduction and development 58, 33-37.
319 Stanton, J.B., Knowles, D.P., O'Rourke, K.I., Herrmann-Hoesing, L.M., Mathison, B.A., Baszler, T.V.,
320 2008. Small-ruminant lentivirus enhances PrPSc accumulation in cultured sheep microglial
321 cells. Journal of virology 82, 9839-9847.
322 Stengel, A., Bach, C., Vorberg, I., Frank, O., Gilch, S., Lutzny, G., Seifarth, W., Erfle, V., Maas, E.,
323 Schatzl, H., Leib-Mosch, C., Greenwood, A.D., 2006. Prion infection influences murine
324 endogenous retrovirus expression in neuronal cells. Biochemical and biophysical research
325 communications 343, 825-831.
326 Taruscio, D., Mantovani, A., 2004. Factors regulating endogenous retroviral sequences in human and
327 mouse. Cytogenetic and genome research 105, 351-362.
328 Young, G.R., Mavrommatis, B., Kassiotis, G., 2014. Microarray analysis reveals global modulation of
329 endogenous retroelement transcription by microbes. Retrovirology 11, 59.
330 Zeng, M., Hu, Z., Shi, X., Li, X., Zhan, X., Li, X.D., Wang, J., Choi, J.H., Wang, K.W., Purrington, T., Tang,
331 M., Fina, M., DeBerardinis, R.J., Moresco, E.M., Pedersen, G., McInerney, G.M., Karlsson
332 Hedestam, G.B., Chen, Z.J., Beutler, B., 2014. MAVS, cGAS, and endogenous retroviruses in T-
333 independent B cell responses. Science (New York, N.Y.) 346, 1486-1492.

334

335

Figure Legends:

Figure 1: OERV mRNA expression in spleen and prescapular lymph node of mock-infected sheep. OERV expression in samples from prescapular lymph node (PSLN) and spleen (SP) of all mock-infected VRQ/VRQ (VV) and ARR/ARR (AA) sheep was analysed by RT-qPCR. For each genotype and tissue, the scatter plot shows ΔCt values (difference between Ct values for gene of interest and reference gene) for individual animals, along with mean ± standard deviation for the group.

Figure 2: **OERV mRNA expression in the prescapular lymph node of scrapie-infected sheep.** OERV mRNA expression in PSLN of susceptible VRQ/VRQ (upper panel) and resistant ARR/ARR (lower panel) sheep was analysed by RT-qPCR at different time points following subcutaneous infection with scrapie (SSBP/1). Relative gene expression was calculated in relation to the mean ΔCt value for all mock-infected controls, calibrated to 1. Individual points represent the relative gene expression values for individual mock-infected (open circles) and scrapie-infected (filled circles) sheep, and bars represent the mean value and standard deviation) for the group. (*p* values, * = <0.05, ** = <0.005)

Figure S1: OERV mRNA expression in lymphoid tissues of mock-infected control sheep over the time course of the experiment. Individual points represent the ΔCt values for PSLN (circles) and spleen (squares) samples from individual mock-infected VRQ/VRQ (VV; closed symbols) and ARR/ARR sheep (AA; open symbols) at the time points indicated.

Figure S2: OERV mRNA expression in the spleen of scrapie-infected sheep. OERV mRNA expression in spleen of susceptible VRQ/VRQ (upper panel) and resistant ARR/ARR (lower panel) sheep was analysed by RT-qPCR at different time points following subcutaneous infection with scrapie (SSBP/1). CS denotes samples taken at clinical stage of disease. Relative gene expression was calculated in relation to the mean ΔCt value for all mock-infected controls, calibrated to 1. Individual points represent the relative gene expression values for individual mock-infected (open circles) and scrapie-infected (filled circles) sheep, and bars represent the mean value and standard deviation) for the group. (*p* values, * = <0.05, ** = <0.005, *** = <0.0005)

Figure 1:

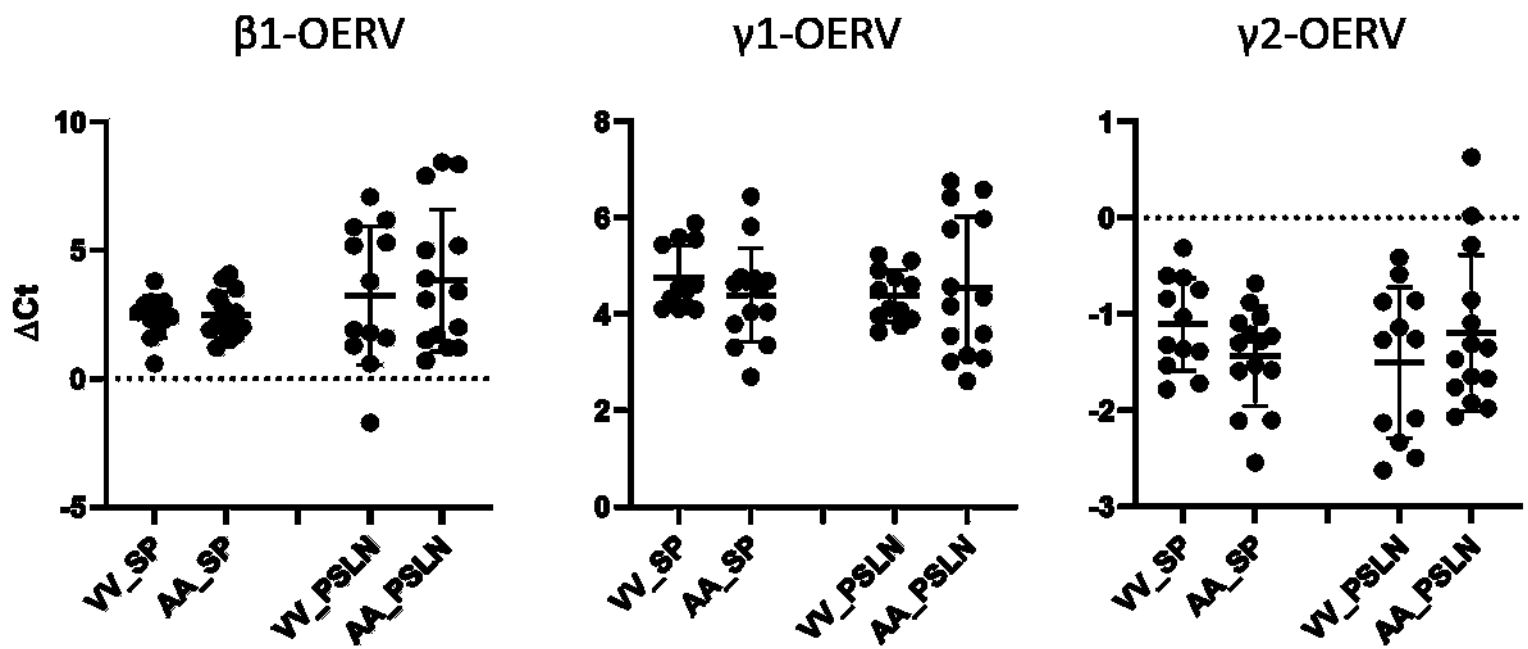
β1-OERV
γ1-OERV
γ2-OERV
ΔCt
10
5
0
-5
8
6
4
2
0
1
0
-1
-2
-3
VV_SP
AA_SP
VV_PSLN
AA_PSLN

Figure 2:

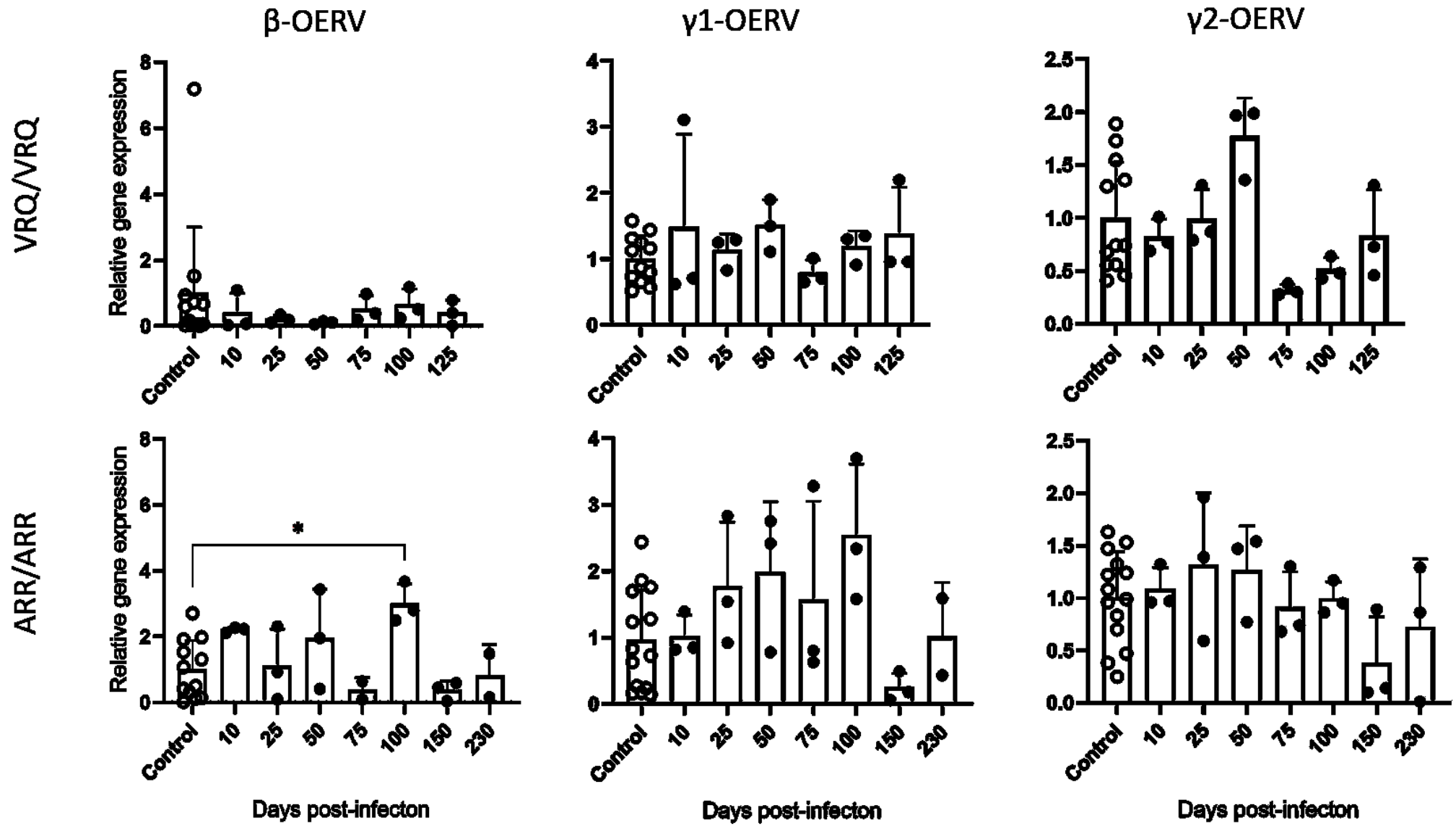
β-OERV
γ1-OERV
γ2-OERV
VRQ/VRQ
ARR/ARR
Relative gene expression
Control
10
25
50
75
100
125
150
230
*
Days post-infecton

Figure S1:

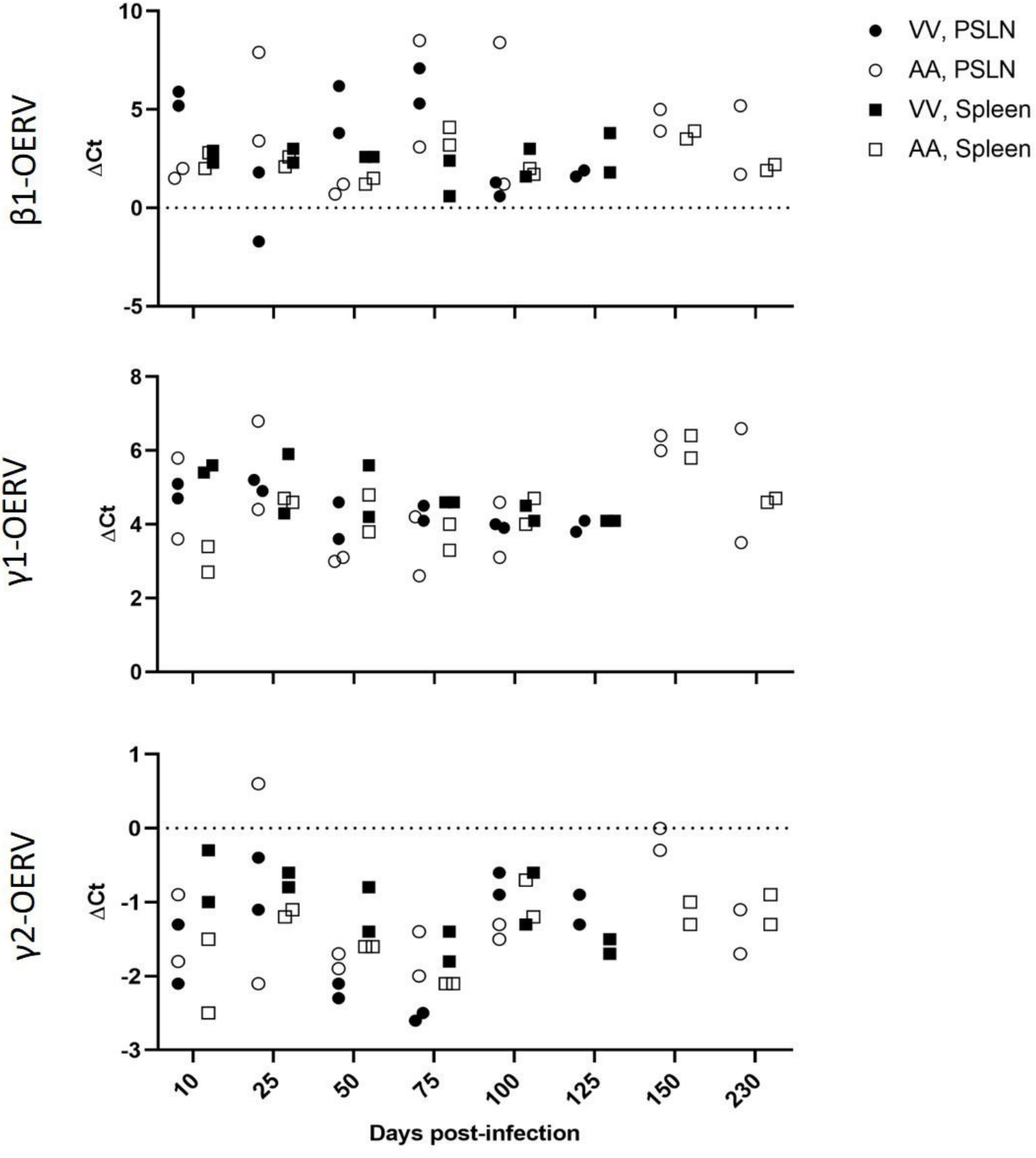
β1-OERV
γ1-OERV
γ2-OERV
ΔCt
10
5
0
-5
8
6
4
2
1
-1
-2
-3
10
25
50
75
100
125
150
230
Days post-infection
VV, PSLN
AA, PSLN
VV, Spleen
AA, Spleen

Figure S2:

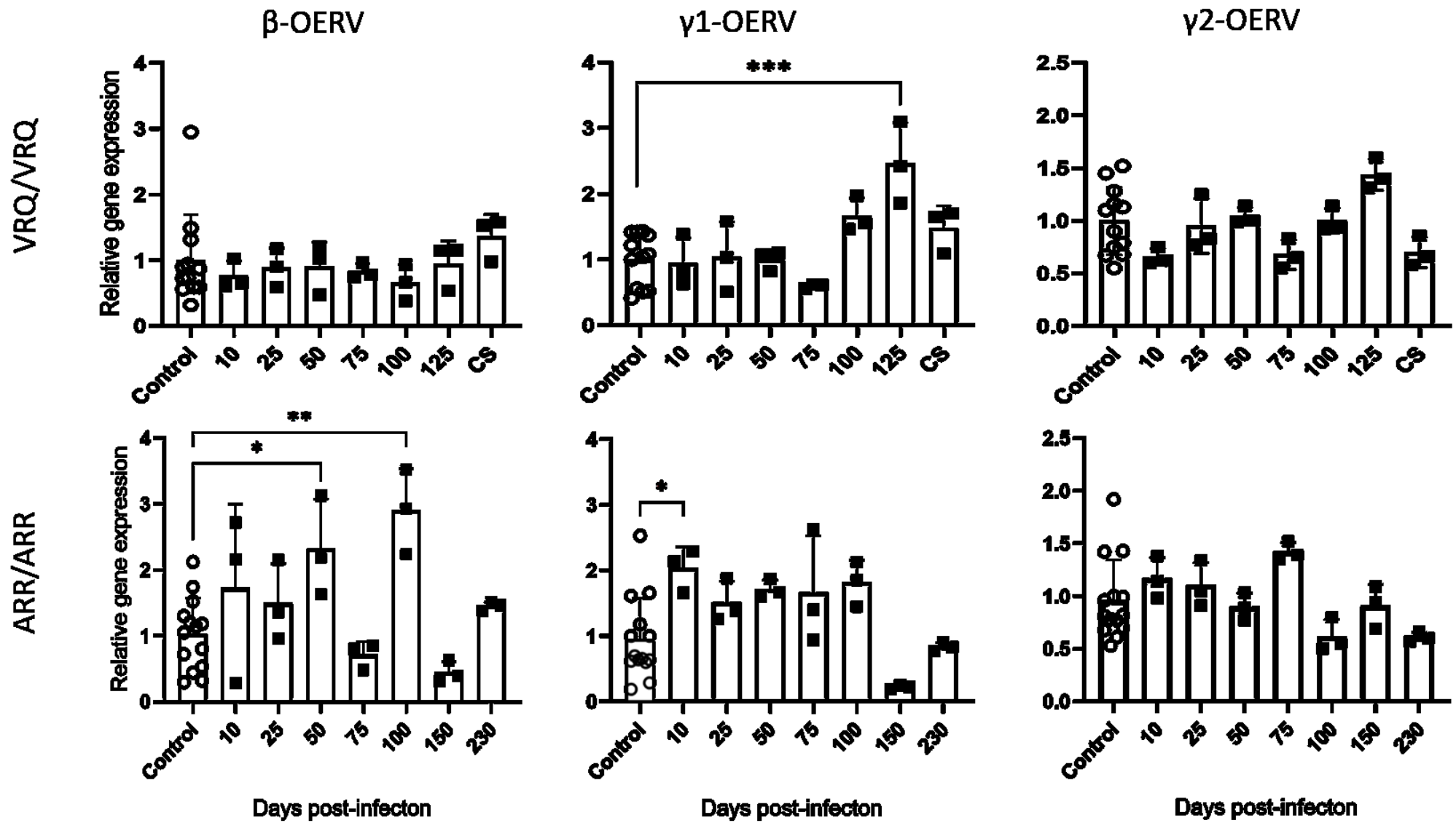
β-OERV
γ1-OERV
γ2-OERV
VRQ/VRQ
ARR/ARR
Relative gene expression
Control
10
25
50
75
100
125
CS
150
230
***
**
*
Days post-infecton

Supplementary Methods

Experimental infection of sheep with scrapie and tissue collection:

The tissue samples for this study were collected from the animals previously used in a study to look into the progression of scrapie pathology in the peripheral lymphoid system and how scrapie infection affects the transcriptome of the lymph nodes and spleen (Gossner et al., 2011). New Zealand Cheviot sheep of two different *PRNP* genotypes VRQ/VRQ and ARR/ARR were from the DEFRA scrapie-free breeding flock (Houston et al., 2002). All of these sheep were inoculated subcutaneously in the neck region drained by the prescapular lymph node (PSLN) with 2 ml of 10% (w/v) brain homogenate; three sheep for each time point for each genotype were infected with SSBP/1 experimental scrapie and two mock-infected with normal brain homogenate. Highly susceptible (VRQ/VRQ) animals were killed by exsanguination under terminal anaesthesia at 10, 25, 50, 75, 100 and 125 days post-infection (dpi) and at clinical stage of the disease. The same procedure was followed for sheep of the scrapie-resistant genotype (ARR/ARR) with additional time points at 150 and 230 dpi. Since ARR/ARR animals are resistant to scrapie, there was no clinical group for this genotype. Animal experiments were performed under an Animals (Scientific Procedures) Act 1986 Project Licence PPL 60/02192. Animals were killed by exsanguination under terminal anaesthesia and tissues were removed immediately post mortem. Dissected tissues were stored in RNAlater (Ambion, Huntingdon, UK) at −80 °C.

RNA extraction and cDNA synthesis:

Total RNA from spleen and prescapular lymph nodes was extracted using the RiboPure kit (Ambion). RNA was digested with DNAse I (Qiagen) to remove any remaining genomic DNA from sample and was then cleaned up using RNeasy MinElute Cleanup Kit (Qiagen). RNA was quantified using a NanoDrop ND-1000 spectrophotometer and quality was assessed using RNA 6000 Nano LabChip on the Agilent 2100 bioanalyzer. First strand cDNA synthesis was performed with 1µg of total RNA using 150ng random hexamer primers (Promega), 100 U SuperScript® III Reverse Transcriptase (Invitrogen, Paisley, UK), 5X RT buffer, 20 U RNasin Plus RNase inhibitor (Promega) and 0.1M DTT (Invitrogen, Paisley, UK) in a final volume of 10 µl. RNA (also no RT (Reverse Transcriptase) control) were diluted to a similar concentration (25ng/µl), quantified with NanoDrop.

RT-qPCR assay:

Two-step RT-qPCR was performed using FastStart Universal SYBR Green Master (Rox) (Roche, Germany) and Mx3000P qPCR system (Stratagene, Agilent technologies, USA). Primers used (Table 1) for endogenous retroviral amplification were those already published (Black et al., 2010; Klymiuk et al., 2003). Briefly, the primers for β1-OERV amplified *env* and the U3 region of the LTRs of the enJSRV genome whereas those for γ-OERV amplified the *pro*/*pol* region. Primers were synthesized from Eurofins (Wolverhampton, UK). The presence of gene specific single band amplification was also confirmed by 1.2% agarose gel electrophoresis using SYBR® Safe DNA gel stain (Invitrogen, Paisley, UK). Reference genes selected (SDHA and YWHAZ) are already screened and published (Gossner et al., 2009). Genomic DNA contamination was assessed using an identical reaction without RT and no template control was used as negative control.

All reactions were performed in a 20µl final volume containing 2µl (50ng) template cDNA (synthesized from 1µg (100ng/µl) of total RNA and then diluted to 25ng/µl for RT-qPCR, assuming all RNA is converted into cDNA) or no RT negative control, 10 µl of 2X FastStart SYBR Green Master (Roche Diagnostics Ltd., Lewes, UK), 1.2 µl of each primer at optimum concentrations (300nM) and 5.6µl nuclease-free water. Sheep genomic DNA as positive and NTC (no template control) as negative control were used in each run. The amplification profile used was the same for all genes; 10 min at 95°C, followed by 40 cycles of 30 s at 95°C, 60 s at 60°C and 60s at 72°C, followed by dissociation curve analysis to confirm a single gene product.

Relative expression levels were quantified from at least two different cDNA preparations in separate RT-qPCR runs, each time using cDNA from a different RT reaction and within a run; each sample was assayed in duplicate. The Ct values were normalized to the levels of the reference genes. Gene expression levels were quantified using ΔΔCt method. Since the background messenger RNA expression levels in mock-infected negative control did not show any clear trend over time, we grouped all controls for the ease of comparison. We normalized the gene expression data from all mock-infected control sheep to 1 and then compared with infected animals for a given time point to calculate fold change. All samples of a time point for a tissue were run on the same plate.

Supplementary Tables

Supplementary Table S1

Primer sequences used for RT-qPCR

Gene	Primer Sequence 5'- 3'	Amplicon Size (bp)
enJSRVs env / β1	**F:** GRYTTTCCRTGGGATAAGGTGAA **R:** ACAATCACYAGACCCTTACCATTG	616
γ1-OERV *pro*/*pol*	**F:** GACAACCAATTCATGTTTTAT **R:** GGTACTCACAGAGATCTTCGC	654
γ2-OERV *pro*/*pol*	**F:** GACTACAAAACGGCATGTGAA **R:** GCGAGTTTTTGAAACCCTGTG	770
SDHA	**F:** ACCTGATGCTTTGTGCTCTGC **R:** CCTGGATGGGCTTGGAGTAA	126

Supplementary table S1. The reference genes SDHA was used for normalization with cDNA derived from the spleen and prescapular lymph node samples.

Table S2: Linear regression model summary for negative control animals

								ANOVA for regression		
Genotype	**Tissue**	**OERV**	**Model**	**Regression coefficient (β)**	**Standard Error (S.E)**	**t**	***p*-value**	**F**	***p*-value**	***R^2***
VRQ/VRQ	**Spleen**	β-OERV	Constant	2.49	0.461	5.398	<0.001	0.044	0.838	0.004
			Time	-0.001	0.006	-0.21	0.838			
		γ1-OERV	Constant	5.497	0.267	20.601	0	10.938	0.008*	0.522
			Time	-0.012	0.004	-3.307	0.008*			
		γ2-OERV	Constant	-0.637	0.213	-2.991	0.014	6.595	0.028*	0.397
			Time	-0.007	0.003	-2.568	0.028*			
	PSLN	β-OERV	Constant	0.607	0.473	1.284	0.228	0.181	0.68	0.018
			Time	-0.03	0.006	-0.425	0.68			
		γ1-OERV	Constant	0.033	0.007	4.939	0.001	9.673	0.011*	0.492
			Time	<0.001	<0.001	3.11	0.011*			
		γ2-OERV	Constant	3.609	0.918	3.931	0.003	0.214	0.634	0.024
			Time	-0.006	0.012	-0.491	0.634			
ARR/ARR	**Spleen**	β-OERV	Constant	2.353	0.404	5.82	<0.001	0.156	0.7	0.013
			Time	0.001	0.003	0.395	0.7			
		γ1-OERV	Constant	3.77	0.374	10.069	<0.001	4.462	0.056	0.271
			Time	0.007	0.003	2.112	0.056			
		γ2-OERV	Constant	-1.723	0.204	-8.447	<0.001	3.187	0.1	0.21
			Time	0.003	0.002	1.785	0.1			
	PSLN	β-OERV	Constant	3.51	1.248	2.812	0.016	0.11	0.746	0.009
			Time	0.004	0.011	0.331	0.746			
		γ1-OERV	Constant	4.143	0.657	6.306	<0.001	0.617	0.447	0.049
			Time	0.004	0.006	0.786	0.447			
		γ2-OERV	Constant	-1.343	0.364	-3.689	0.003	0.184	0.676	0.015
			Time	0.001	0.003	0.676	0.676			

* p-value < 0.05

References

Black, S.G., Arnaud, F., Burghardt, R.C., Satterfield, M.C., Fleming, J.A., Long, C.R., Hanna, C., Murphy, L., Biek, R., Palmarini, M., Spencer, T.E., 2010. Viral particles of endogenous betaretroviruses are released in the sheep uterus and infect the conceptus trophectoderm in a transspecies embryo transfer model. Journal of virology 84, 9078-9085.

Gossner, A., Roupaka, S., Foster, J., Hunter, N., Hopkins, J., 2011. Transcriptional profiling of peripheral lymphoid tissue reveals genes and networks linked to SSBP/1 scrapie pathology in sheep. Veterinary microbiology 153, 218-228.

Gossner, A.G., Bennet, N., Hunter, N., Hopkins, J., 2009. Differential expression of Prnp and Sprn in scrapie infected sheep also reveals Prnp genotype specific differences. Biochemical and biophysical research communications 378, 862-866.

Houston, E.F., Halliday, S.I., Jeffrey, M., Goldmann, W., Hunter, N., 2002. New Zealand sheep with scrapie-susceptible PrP genotypes succumb to experimental challenge with a sheep-passaged scrapie isolate (SSBP/1). The Journal of general virology 83, 1247-1250.

Klymiuk, N., Muller, M., Brem, G., Aigner, B., 2003. Characterization of endogenous retroviruses in sheep. Journal of virology 77, 11268-11273.

Spleen

		Beta				p value		G1				p value	
	Negative cont	ΔCt	Log2 conv	0.22	Fold change	Anova	Tukey's	Negative controls	ΔCt	Log2 conv	0.04	Fold chang	Anova	Tukey's
Negative	10dpi	2.3	0.20	0.90	1.00			10dpi	5.6	0.02	0.51	1.0		
		2.9	0.13	0.59					5.4	0.02	0.56			
	25dpi	3.0	0.12	0.56				25dpi	5.9	0.02	0.41			
		2.3	0.21	0.94					4.3	0.05	1.22			
	50dpi	2.6	0.16	0.74				50dpi	4.2	0.06	1.37			
		2.6	0.16	0.73					5.6	0.02	0.52			
	75dpi	2.4	0.19	0.87				75dpi	4.6	0.04	1.04			
		0.6	0.65	2.95					4.6	0.04	1.00			
	100dpi	1.6	0.33	1.49				100dpi	4.5	0.04	1.08			
		3.0	0.13	0.59					4.1	0.06	1.42			
	125dpi	1.8	0.29	1.31				125dpi	4.1	0.06	1.42			
		3.8	0.07	0.32					4.1	0.06	1.43			
	Infected							Infected						
Infected	10dpi	2.8	0.14	0.65	0.76	0.79		10dpi	5.3	0.03	0.63	0.9	<.001	1.00
		2.9	0.13	0.61					4.2	0.06	1.38			
		2.2	0.22	1.02					4.9	0.03	0.82			
	25dpi	3.0	0.13	0.59	0.89			25dpi	5.6	0.02	0.51	1.0		1.00
		1.9	0.26	1.18					4.6	0.04	1.03			
		2.3	0.20	0.90					4.0	0.06	1.58			
	50dpi	2.2	0.22	1.02	0.90			50dpi	4.9	0.03	0.82	1.0		1.00
		3.3	0.10	0.47					4.5	0.04	1.10			
		1.9	0.26	1.20					4.5	0.04	1.07			
	75dpi	2.5	0.17	0.78	0.83			75dpi	5.3	0.03	0.62	0.6		0.73
		2.6	0.16	0.75					5.3	0.02	0.61			
		2.3	0.21	0.96					5.5	0.02	0.56			
	100dpi	3.6	0.08	0.38	0.66			100dpi	4.0	0.06	1.55	1.7		0.29
		2.3	0.20	0.93					3.6	0.08	1.97			
		2.8	0.15	0.66					4.1	0.06	1.46			
	125dpi	3.1	0.12	0.54	0.94			**125dpi**	3.3	0.10	2.42	2.5		**<0.001**
		2.0	0.25	1.15					3.7	0.08	1.86			
		2.0	0.25	1.14					3.0	0.13	3.10			
	nical samp	2.2	0.21	0.98	1.36			Clinical samples	4.5	0.04	1.09	1.5		0.64
		1.5	0.35	1.58					3.9	0.07	1.65			
		1.6	0.34	1.53					3.9	0.07	1.70			

Spleen

		Beta				p value		G1				p value	
	Negative cont	ΔCt	Log2 conv	0.21	Fold change	Anova	Tukey's	Negative controls	ΔCt	Log2 conv	0.06	Fold chang	Anova	Tukey's
Negative	10dpi	2.8	0.15	0.70	1.00			10dpi	2.7	0.15	2.66	1.00		
		2.0	0.24	1.15					3.4	0.10	1.69			
	25dpi	2.1	0.23	1.11				25dpi	4.6	0.04	0.73			
		2.6	0.16	0.78					4.7	0.04	0.65			
	50dpi	1.2	0.44	2.07				50dpi	3.8	0.07	1.24			
		1.5	0.36	1.70					4.8	0.04	0.63			
	75dpi	4.1	0.06	0.28				75dpi	4.0	0.06	1.05			
		3.2	0.11	0.52					3.3	0.10	1.74			
	100dpi	2.0	0.25	1.17				100dpi	4.7	0.04	0.67			
		1.7	0.31	1.48					4.0	0.06	1.05			
	150dpi	3.9	0.07	0.31				150dpi	6.4	0.01	0.20			
		3.5	0.09	0.43					5.8	0.02	0.31			
	230dpi	1.9	0.27	1.27				230dpi	4.6	0.04	0.69			
		2.2	0.22	1.03					4.7	0.04	0.67			
	Infected							Infected						
Infected	10dpi	1.2	0.45	2.11	1.68	<0.001	0.605	**10dpi**	2.8	0.14	2.42	2.14	0.001	**0.043**
		0.8	0.56	2.65					2.9	0.13	2.25			
		4.1	0.06	0.28					3.3	0.10	1.75			
	25dpi	2.3	0.20	0.94	1.46		0.925	25dpi	3.6	0.08	1.46	1.59		0.721
		1.8	0.28	1.32					3.7	0.08	1.33			
		1.2	0.44	2.10					3.1	0.11	1.98			
	50dpi	1.2	0.45	2.14	2.26		**0.043**	50dpi	3.3	0.10	1.76	1.80		0.317
		1.6	0.34	1.59					3.4	0.10	1.68			
		0.6	0.64	3.05					3.1	0.11	1.97			
	75dpi	3.4	0.10	0.46	0.69		0.993	75dpi	4.1	0.06	0.99	1.75		0.317
		2.6	0.17	0.79					3.6	0.09	1.48			
		2.5	0.18	0.83					2.6	0.16	2.76			
	100dpi	0.7	0.60	2.86	2.83		**0.001**	100dpi	3.5	0.09	1.53	1.91		0.176
		0.5	0.72	3.44					2.9	0.13	2.25			
		1.1	0.46	2.18					3.2	0.11	1.95			
	150dpi	3.6	0.08	0.38	0.43		0.784	150dpi	6.2	0.01	0.23	0.23		0.341
		4.0	0.06	0.30					6.0	0.02	0.27			
		2.9	0.13	0.62					6.4	0.01	0.20			
	230dpi	1.7	0.30	1.42	1.41		0.957	230dpi	4.2	0.05	0.95	0.88		1.000
		1.8	0.28	1.35					4.4	0.05	0.81			
		1.7	0.31	1.47					4.3	0.05	0.87			

VRQ/VRQ

	G2				*p* value	
Negative cont	ΔCt	Log2 conv	2.26	Fold chang	Anova	Tukey's
10dpi	-0.3	1.24	0.55	1.0		
	-1.0	2.04	0.90			
25dpi	-0.6	1.52	0.67			
	-0.8	1.68	0.75			
50dpi	-1.4	2.62	1.16			
	-0.8	1.79	0.79			
75dpi	-1.4	2.56	1.13			
	-1.8	3.43	1.52			
100dpi	-0.6	1.54	0.68			
	-1.3	2.49	1.10			
125dpi	-1.5	2.89	1.28			
	-1.7	3.28	1.45			
Infected						
10dpi	-0.5	1.40	0.62	0.7	0.009	0.38
	-0.4	1.35	0.60			
	-0.8	1.69	0.75			
25dpi	-0.8	1.74	0.77	1.0		1.00
	-0.9	1.88	0.83			
	-1.5	2.82	1.25			
50dpi	-1.2	2.26	1.00	1.0		1.00
	-1.4	2.58	1.14			
	-1.2	2.23	0.99			
75dpi	-0.9	1.86	0.83	0.7		0.44
	-0.3	1.23	0.55			
	-0.6	1.47	0.65			
100dpi	-1.1	2.08	0.92	1.0		1.00
	-1.4	2.58	1.14			
	-1.1	2.13	0.94			
125dpi	-1.6	2.96	1.31	1.4		0.14
	-1.7	3.15	1.40			
	-1.9	3.61	1.60			
Clinical samp	-0.4	1.31	0.58	0.7		0.55
	-0.6	1.49	0.66			
	-1.0	1.94	0.86			

	Beta				*p* value	
Negative cont	ΔCt	Log2 conv	0.44	Fold chang	Anova	Tukey's
10dpi	5.9	0.02	0.04	1.00		
	5.2	0.03	0.06			
25dpi	1.8	0.29	0.67			
	-1.7	3.17	7.19			
50dpi	3.8	0.07	0.16			
	6.2	0.01	0.03			
75dpi	7.1	0.01	0.02			
	5.3	0.03	0.06			
100dpi	0.6	0.67	1.52			
	1.3	0.41	0.93			
125dpi	1.6	0.32	0.73			
	1.9	0.26	0.59			
Infected						
10dpi	5.1	0.03	0.07	0.40	0.939	
	1.1	0.48	1.09			
	6.2	0.01	0.03			
25dpi	3.7	0.08	0.18	0.21		
	4.6	0.04	0.10			
	2.7	0.15	0.35			
50dpi	4.0	0.06	0.15	0.10		
	5.4	0.02	0.05			
	4.4	0.05	0.11			
75dpi	2.5	0.17	0.39	0.52		
	1.2	0.43	0.98			
	3.5	0.09	0.20			
100dpi	3.2	0.11	0.24	0.64		
	0.9	0.52	1.18			
	2.2	0.22	0.51			
125dpi	2.5	0.18	0.40	0.40		
	8.5	0.00	0.01			
	1.5	0.35	0.79			

ARR/ARR

	G2				*p* value	
Negative cont	ΔCt	Log2 conv	2.89	Fold chang	Anova	Tukey's
10dpi	-2.5	5.80	2.01	1.00		
	-1.5	2.89	1.00			
25dpi	-1.1	2.12	0.74			
	-1.2	2.34	0.81			
50dpi	-1.6	2.98	1.03			
	-1.6	3.00	1.04			
75dpi	-2.1	4.27	1.48			
	-2.1	4.32	1.50			
100dpi	-0.7	1.61	0.56			
	-1.2	2.31	0.80			
150dpi	-1.3	2.46	0.85			
	-1.0	2.04	0.71			
230dpi	-1.3	2.43	0.84			
	-0.9	1.84	0.64			
Infected						
10dpi	-1.6	2.95	1.02	1.22	0.035	0.95
	-1.8	3.43	1.19			
	-2.1	4.16	1.44			
25dpi	-1.5	2.73	0.95	1.15		0.99
	-2.0	4.03	1.40			
	-1.7	3.16	1.09			
50dpi	-1.4	2.69	0.93	0.94		1.00
	-1.6	3.12	1.08			
	-1.2	2.31	0.80			
75dpi	-2.0	4.06	1.41	1.48		0.25
	-2.1	4.20	1.45			
	-2.2	4.56	1.58			
100dpi	-0.7	1.67	0.58	0.65		0.61
	-1.3	2.42	0.84			
	-0.6	1.52	0.53			
150dpi	-1.7	3.27	1.13	0.95		1.00
	-1.1	2.08	0.72			
	-1.5	2.84	0.98			
230dpi	-0.8	1.73	0.60	0.64		0.58
	-0.9	1.81	0.63			
	-1.0	1.99	0.69			

	Beta				*p* value	
Negative cont	ΔCt	Log2 conv	0.19	Fold chang	Anova	Tukey's
10dpi	1.5	0.35	1.78	1.00		
	2.0	0.24	1.25			
25dpi	3.4	0.09	0.48			
	7.9	0.00	0.02			
50dpi	0.7	0.61	3.15			
	1.2	0.43	2.22			
75dpi	8.5	0.00	0.01			
	3.1	0.11	0.59			
100dpi	8.4	0.00	0.02			
	1.2	0.45	2.31			
150dpi	3.9	0.07	0.34			
	5.0	0.03	0.16			
230dpi	5.2	0.03	0.14			
	1.7	0.30	1.53			
Infected						
10dpi	1.1	0.48	2.46	2.6	0.004	0.26
	1.0	0.51	2.60			
	1.0	0.51	2.64			
25dpi	5.5	0.02	0.11	1.3		1.00
	2.3	0.21	1.08			
	0.9	0.52	2.69			
50dpi	3.4	0.09	0.48	2.3		0.54
	1.2	0.44	2.28			
	0.4	0.78	3.99			
75dpi	5.7	0.02	0.10	0.3		0.95
	9.5	0.00	0.01			
	2.8	0.14	0.74			
100dpi	0.7	0.64	3.26	3.5		**0.01**
	0.3	0.83	4.28			
	0.8	0.56	2.90			
150dpi	6.9	0.01	0.04	0.4		0.98
	3.3	0.10	0.52			
	2.9	0.13	0.69			
230dpi	***#VALUE!***	***#VALUE!***	***#VALUE!***	1.0		1.00
	4.9	0.03	0.17			
	1.6	0.34	1.73			

PSLN

	G1				*p* value		G2				*p* value	
Negative cont	ΔCt	Log2 conv	0.05	Fold chang	Anova	Tukey's	Negative cont	ΔCt	Log2 conv	3.24	Fold chang	Anova	Tukey's
10dpi	4.7	0.04	0.73	1.0			10dpi	-1.3	2.40	0.74	1.0		
	5.1	0.03	0.57					-2.1	4.22	1.30			
25dpi	5.2	0.03	0.52				25dpi	-1.1	2.20	0.68			
	4.9	0.03	0.65					-0.4	1.33	0.41			
50dpi	3.6	0.08	1.58				50dpi	-2.3	5.03	1.55			
	4.6	0.04	0.80					-2.1	4.38	1.36			
75dpi	4.5	0.04	0.87				75dpi	-2.5	5.60	1.73			
	4.1	0.06	1.13					-2.6	6.13	1.89			
100dpi	4.0	0.06	1.25				100dpi	-0.6	1.50	0.46			
	3.9	0.07	1.31					-0.9	1.82	0.56			
125dpi	4.1	0.06	1.16				125dpi	-0.9	1.82	0.56			
	3.8	0.07	1.44					-1.3	2.40	0.74			
Infected							**Infected**						
10dpi	5.0	0.03	0.62	1.5	0.467		10dpi	-1.2	2.25	0.69	0.8	0.010	0.99
	2.7	0.16	3.11					-1.3	2.49	0.77			
	4.8	0.04	0.71					-1.7	3.28	1.01			
25dpi	4.0	0.06	1.25	1.1			25dpi	-2.1	4.24	1.31	1.0		1.00
	4.6	0.04	0.83					-1.5	2.82	0.87			
	3.9	0.07	1.29					-1.3	2.54	0.79			
50dpi	3.7	0.08	1.50	1.5			50dpi	-2.1	4.38	1.36	1.8		0.11
	4.1	0.06	1.11					-2.7	6.43	1.99			
	3.4	0.10	1.90					-2.7	6.36	1.97			
75dpi	4.8	0.04	0.70	0.8			75dpi	0.1	0.96	0.30	0.3		0.19
	4.3	0.05	1.01					-0.3	1.22	0.38			
	4.9	0.03	0.65					0.1	0.92	0.28			
100dpi	4.4	0.05	0.91	1.2			100dpi	-0.6	1.56	0.48	0.5		0.57
	3.9	0.07	1.35					-1.1	2.08	0.64			
	3.9	0.07	1.30					-0.5	1.39	0.43			
125dpi	3.2	0.11	2.20	1.4			125dpi	-1.2	2.37	0.73	0.8		1.00
	4.3	0.05	0.96					-0.6	1.49	0.46			
	4.3	0.05	0.96					-2.1	4.24	1.31			

PSLN

	G1				*p* value		G2				*p* value	
Negative cont	ΔCt	Log2 conv	0.06	Fold chang	Anova	Tukey's	Negative cont	ΔCt	Log2 conv	2.57	Fold chang	Anova	Tukey's
10dpi	3.6	0.08	1.29	1.00			10dpi	-1.8	3.39	1.32	1.00		
	5.8	0.02	0.28					-0.9	1.80	0.70			
25dpi	4.4	0.05	0.76				25dpi	-2.1	4.18	1.63			
	6.8	0.01	0.14					0.6	0.65	0.25			
50dpi	3.1	0.11	1.77				50dpi	-1.9	3.77	1.47			
	3.0	0.12	1.93					-1.7	3.14	1.22			
75dpi	4.2	0.06	0.86				75dpi	-1.4	2.55	0.99			
	2.6	0.16	2.54					-2.0	3.94	1.53			
100dpi	4.6	0.04	0.66				100dpi	-1.3	2.47	0.96			
	3.1	0.12	1.84					-1.5	2.77	1.08			
150dpi	6.0	0.02	0.25				150dpi	0.02	0.99	0.38			
	6.4	0.01	0.18					-0.3	1.21	0.47			
230dpi	6.6	0.01	0.16				230dpi	-1.1	2.13	0.83			
	3.5	0.09	1.33					-1.7	3.18	1.24			
Infected							**Infected**						
10dpi	4.2	0.05	0.85	1.06	0.046	1.000	10dpi	-1.3	2.46	0.96	1.08	0.256	
	4.1	0.06	0.89					-1.3	2.49	0.97			
	3.4	0.09	1.45					-1.8	3.39	1.32			
25dpi	4.0	0.06	0.95	1.84		0.833	25dpi	-0.6	1.51	0.59	1.31		
	3.3	0.10	1.60					-2.3	5.05	1.96			
	2.4	0.19	2.95					-1.8	3.58	1.39			
50dpi	4.3	0.05	0.81	2.06		0.626	50dpi	-1.0	1.97	0.77	1.26		
	2.4	0.18	2.86					-2.0	3.96	1.54			
	2.6	0.16	2.52					-1.9	3.77	1.47			
75dpi	4.2	0.05	0.83	1.63		0.958	75dpi	-0.9	1.89	0.74	0.91		
	4.6	0.04	0.65					-0.8	1.75	0.68			
	2.2	0.22	3.41					-1.7	3.35	1.30			
100dpi	3.2	0.11	1.64	2.65		0.095	100dpi	-1.3	2.45	0.95	0.99		
	2.7	0.16	2.44					-1.1	2.21	0.86			
	2.0	0.25	3.86					-1.6	3.01	1.17			
150dpi	8.1	0.00	0.06	0.25		0.851	150dpi	1.5	0.36	0.14	0.38		
	6.4	0.01	0.19					2.0	0.26	0.10			
	4.9	0.03	0.51					-1.2	2.28	0.89			
230dpi	***#VALUE!***	***#VALUE!***	***#VALUE!***	1.05		1.000	230dpi	5.4	0.02	0.01	0.72		
	5.1	0.03	0.45					-1.2	2.22	0.86			
	3.2	0.11	1.66					-1.7	3.32	1.29			